Mechanical understanding of hunting waves generated by killer whales

You, Hojung; Hwang, Jin Hwan; Park, Yong Sung

Published in:
Marine Mammal Science

DOI:
10.1111/mms.12600

Publication date:
2019

Document Version
Peer reviewed version

Mechanical understanding of hunting waves generated by killer whales

Hojung You, Jin Hwan Hwang, Yong Sung Park

Institutions

[1]Department of Civil & Environmental Engineering, Seoul National University, Gwanak-ro, Gwanak-gu, Seoul 08826 Republic of Korea

[2]Institute of Construction & Environmental engineering, Seoul National University, Gwanak-ro, Gwanak-gu, Seoul 08826 Republic of Korea

[3] School of Science & Engineering, University of Dundee, Dundee DD1 4HN, U.K;

[*]Corresponding author: jinhwang@snu.ac.kr

Short Title:

Word Count: [Insert Word Count text here]

Corresponding Author: Jin Hwan Hwang, email: jinhwang@snu.ac.kr, Associate professor, Institute of construction and environmental engineering

Abstract

The ‘wave wash’ hunting technique of killer whales (*Orcinus orca*) is unique in that they hunt a prey located outside of the water by generating waves. For the quantitative analysis of the specific hunting mechanism of ‘wave wash’, data are acquired from computational fluid dynamics (CFD) technique and the wave theory is introduced as theoretical background for explanation of that mechanism. The relationships between swimming characteristics and wave parameters are first defined. The numerical investigation shows that wavelength increases linearly as swimming speed increases and the wave height also increases as swimming speed increases and the depth of swimming becomes shallower, and later converges to maximum value, 2.42 m. The success of hunting is determined by two wave parameters which indicate the intensity of ‘wave wash’; the wave height and the force imposed on prey. The metabolic rate and the drag force, which indicates the efficiency of the locomotion, vary by the swimming speed (V) and swimming depth (d) of killer whales. To generate successful hunting waves with less effort, the optimal ranges of swimming characteristics are estimated as 3 m/s $\leq V \leq$ 5 m/s and 0.5 m $\leq d \leq$ 1.1 m.

Key words: Killer whales, hunting wave, swimming speed, swimming depth.

Flow controls of aquatic animals demonstrate that they have evolved to utilize fluid dynamics optimizing behaviors (Fish and Lauder 2006), which also can be seen in hunting strategies. As an example, suction-feeding behavior in fish and mammals show that they are able to actively control inflow velocity by changing their mouth size and the elevation of the rostrum (Wilga *et al*. 2012). Harbor seals passively detect the location of prey with their sensitive whiskers by tracking the vortex structure created behind swimming fish (Dehnhardt *et al.* 2001). In general, hunting strategies in animals have evolved to achieve the maximum probability of success with less effort, and in particular aquatic mammals have their own hunting techniques to take the advantage of living in a fluid.

Killer whales (*Orcinus orca*, denoted hereinafter *O. orca*) are predators of other marine species and their diverse hunting mechanisms have been studied by numerous researchers (Jefferson *et al.* 1991, Guinet 1990, Guinet and Bouvier 2004, Guinet *et al.* 2007, Ford 2005, Pitman *et al.* 2001, Reyes and Borboroglu 2004, Baird and Dill 1995). The most common strategy is 'chase and attack' which accompanies tireless swimming that lasts for more than 30 min to hunt prey in the water. 'Wave wash' is a unique hunting tactic to generate large surface waves to hunt prey outside of water, usually lying on the floating ice by making the prey slide from the ice into the water (Pitman and Ensor 2003, Visser *et al.* 2008). This strategy only requires sudden acceleration of swimming lasting for few seconds. Their active manipulation of the marine environment extends the realm of where they can hunt prey, including the frozen surface of the water.

Compared to other species of cetaceans, *O. orca* exhibit high-level swimming performances (*i.e*., high speed, high efficiency) (Fish 1998), which substantially change the hydrodynamics along the swimming trajectory. When *O. orca* swim near the water surface, kinematic energy created by the swimming converts into potential energy of surface waves (Fish 2000). The

whole procedures of 'wave wash' technique of *O. orca*; which include breaking the large ice floe into smaller pieces, tilting the floe and finally washing away the prey (Visser *et al.* 2008), rely on the surface wave generated by swimming *O. orca*. This wave is going to be named hereafter as 'hunting wave' in this study.

Previous studies that focused on the influence of ocean waves on marine environment considered the wave periods, lengths, heights and the shapes as the main parameters to analyze (Bonham 1983, Anderson 2002, Denny 1999). Among those variables, the wave height, which determines the extent of overtopping or run-up (Waal and Meer 1992), is going to be discussed in this study, since wave wash derived by *O. orca* hunting technique results from the overtopping process. The overtopping process occurs when the waves meet the structural obstacles (i.e. ice floe or seals lying on floating ice) of which height is smaller than that of the incoming wave (Alvarellos *et al.* 2017). Hydrodynamic forces of waves imposed on structural obstacles are another parameter to be considered. Sliding of seals beyond the edge of ice floe occurs when wave force exceeds the static friction to result overwash and successful hunting (Buckley *et al.* 2011).

The aim of the precedent research is to assess the efficiency of the 'wave-wash' hunting strategy of *O. orca*. In nature, efficiency plays a crucial role in the survival of species and *O. orca* also endeavor to accomplish the optimization of their behaviors. Swimming is the typical behavior which must be optimized since it is the primary means of locomotion allowed to *O. orca* (Williams 2000). Swimming is considered efficient when drag force which resists the movement of *O. orca* in fluid is reduced (Fish 1998). Many aspects of *O. orca* are designed in this regard such as their streamline body (Fish 2000) and submerged swimming rather than surface swimming (Williams 2000). To define efficient 'wave wash' strategy of *O. orca*, two questions needs to be answered.

1) Do hunting waves exceed required wave height and force to succeed wave wash? (i.e. success and failure of hunting process)

2) What are the ranges of swimming characteristics of *O. orca* to generate successful 'wave wash' with least effort?

Previous studies were focused on deliberate description of 'wave wash' strategy of *O. orca* (Pitman and Ensor 2003, Visser *et al.* 2008), and we endeavor to quantify the wave characteristics and locomotion of *O. orca* to better understand specific 'wave washing' hunting strategy. Based on minimum wave height and force required to achieve successful hunting wave, efficient ranges of swimming velocity and swimming depth are going to be estimated in this research.

Use of computational fluid dynamics method (CFD) enables the analysis of hydrodynamics involved in complex process of marine ethology. 3D simulation of tadpole locomotion (Liu *et al.* 1997) and telemetry tag attached to dolphin (Pavlov *et al.* 2012) testify the capability of CFD as a tool to analyze behaviors of aquatic animals. Hunting waves of *O. orca* are simulated computationally in various conditions to obtain sufficient data needed to investigate the roles of each variable in the hunting mechanism. Ultimate goal of this study is to define an efficient hunting process of *O.* orca based on simulation results and wave theory to establish standards of successful 'wave wash' strategy of *O. orca*.

Methods

Estimation of O. orca properties in nature

Since field observation is unavailable at this moment, good quality video recorded by I. Visser was used to analyze 'wave wash' hunting technique of *O. orca* and we roughly estimated

the whales' swimming speed, the wave height and celerity and the other physical quantities. The segment of video recording is available at http://www.youtube.com/watch?v=VyfOp_keW0A. The reasonable engineering estimations of the speed and depth of swimming are what we are aim to achieve. Although the average values of those two characteristics are revealed in the precedent studies, their ranges during 'overwash' hunting are not quantified well.

As a solution, we estimate the values by engineering assumption based on the video recorded by I. Visser. At 1.14 min of the elapse time, group of *O. orca* initiates swimming from the distance of 2-4 times their own body length away from the ice floe. After 1.17 min, they reach the ice floe and generates hunting wave behind their body to overwash the crab-eater seal lying on the floating ice. Based on the assumption that female adult *O. orca* play the dominant role in hunting (Guinet *et al.* 2007), we can estimate that *O. orca* had swim 11-22 m during 3 seconds by approximating the length of *O. orca* 's body as 5.6 m, the average body length of female *O. orca*. Based on those quantities, the swimming speed would be calculated as be in the range of $3.67 \le V \le 7.33$ m/s. In contrast, the depth of swimming is unavailable to be defined quantitatively even from the careful analysis of the video recording. It is only possible to presume that the *O. orca* swim close to the surface since their locomotion inside water are clearly observed from the video recordings.

Dimensional analysis

Model, which is a scaled version of prototype enables efficient analysis of large scale phenomenon in nature by reducing its size. Law of similitude should be considered to decide suitable dimension of a model and dimensional analysis is a useful tool to analyze the similarity between prototype and model (Street *et al.* 1996).

Primary restoring forces of waves can be either gravity or surface tension based on wave

period (Kinsman 1965). Dynamic similarity is satisfied among natural and modeled systems with different scales when they have identical Froude and Weber number (Alexander and Jayes 1983) considering gravity and surface tension as driving forces of waves,

$$Fr_D = \frac{V}{\sqrt{gD}} \tag{1}$$

$$We = \frac{\rho D V^2}{\sigma} \tag{2}$$

where V is the speed of *O. orca*, D, the characteristic length (i.e. average length of female *O. orca*), g is the gravitational acceleration, ρ is the density of fluid and σ is the surface tension. The observation report of 'wave wash' hunting strategy suggest that majority of *O. orca* involved in hunting are female ($>50\%$) (Visser *et al.* 2008) and nondimensional numbers are computed based on properties of female *O. orca* estimated previously; $3.67 \le V \le 7.33$ m/s and $D = 5.6$ m. Appropriate scale of model is determined when nondimensional numbers of models equals to the prototype.

Table 1. Dimension of prototype and of model to satisfy similar range of the Froude number and the Weber number.

The weber number represent the relative significance between surface tension and inertia forces. If the number is large, it represents the capability of inertia generated by *O. orca* to create the surface wave by overcoming the restoring force, surface tension. In the opposite condition of the small Weber number, surface tension is too dominant to suppress the gravitational restoring force. The large Weber number ($\sim 2.3\times10^6 \gg 1$) of prototype indicates that surface tension is negligible to hunting wave or propagation speed (Tab. 1). When this number is small in model, the surface tension will be overly imposed and become important

factor. Therefore, the Weber number should be large enough to neglect surface tension and the Weber number of model ($\square$ $0.13 \sim 3.29 \times 10^2$ $\square$ 1) satisfy the condition (Tab. 1).

The Froude number is primary measure to evaluate similitude of real nature and model, and two systems should exhibit similar range of the Froude number. Maximum velocity is established as 1.0 m/s in model due to the limitation of experiment devices. It determines the appropriate range of body length of female *O. orca* model as 0.03 - 0.05 m to adjust Froude number, and we selected 0.04 m. Precedent researches report that juveniles reach half of female body size and male reach 1.2 -1.3 times of female body size and their lengths corresponding to models are respectively estimated as 0.02 m and 0.05 m. Based on the assumption that length of *O. orca* and the depth at which *O. orca* swims are in the similar order, the ranges of such depth are established as 0.003 - 0.03 m. The Froude number of prototype and model both exist in the range of 0.2 - 1.2, showing propriety of model to represent prototype (Tab. 1).

Computational Fluid Dynamics (CFD) Modeling and Simulations

The continuity and the Naiver-Stokes equations are generally used to describe the motion of fluid continuum. OpenFOAM is an open source for numerical simulation of flows using the finite volume method solving the equations (Greenshields 2015), and the governing equations for the current problem is.

$$\frac{\partial \rho}{\partial t} + \frac{\partial}{\partial x_i}(\rho u_i) = 0 \tag{3}$$

and

$$\frac{\partial}{\partial t}(\rho u_i) + \frac{\partial}{\partial x_j}(\rho u_j u_i) = -\frac{\partial p}{\partial x_i} + \frac{\partial}{\partial x_j}\mu\left(\frac{\partial u_i}{\partial x_j} + \frac{\partial u_j}{\partial x_i}\right) + \rho g_i + F_i \tag{4}$$

in which u_i is the velocity vector, t is the time, ρ is the fluid density, p is the pressure, F is

body force, and μ is the dynamic viscosity of the fluid. Suffixes i and j can be 1, 2, or 3, denoting components in the x, y, and z directions, respectively. Among turbulence models, Reynolds Average Simulation (RAS), specifically $k-\varepsilon$ model is applied (Lew *et al.* 2001).

To treat the free surface, the present work adopts a solver '*interFoam*' based on 'Volume of Fluid (VOF)' method (Jacobsen *et al.* 2011). In this method, both air and fluid exist together in each cell of grid and the physical properties are calculated with the weighted averages depending on the volume fractions of each component in one cell. Volume fraction is represented as a and ranging from 1 (i.e. full of water) to 0 (i.e. full of air). For a cell including the interface between air and water, a would be between 0 and 1. The transport equation of volume fraction a is expressed as below.

$$\frac{\partial a}{\partial t}+\vec{\nabla}.(a\vec{u})=0 \tag{5}$$

The range of variables applied to CFD simulations encompass *O. orca* length of 0.02 - 0.05 m, velocity at range of 0.15 – 0.75 m/s and swimming depth of 0.003 – 0.03 m. The simulation is based on two-dimensional assumption to efficiently obtain the target wave values; wavelength and wave height.

Geometry and boundary conditions for numerical simulation

The schematic diagram depicts geometry and boundary conditions for numerical simulation selected to analyze 'wave wash' hunting mechanism (Fig.1). The length of flume is decided as 1 - 3 m depending on the wake generated behind *O. orca* for each velocity condition. Mean water level without *O. orca* is 0.10 m for all conditions. Since water depth is deep enough to neglect the bottom friction in the real sea, slip boundary condition is applied to sidewalls and bottom of flume, neglecting the wall friction and eliminating the disparity between the

prototype and the numerical models. Slip boundary condition guarantee uniform velocity profile in the normal direction from the wall by ignoring the wall friction. For upstream inlet, constant flowrate is assigned and the desired velocity is specified at the downstream outlet (Jasak *et al.* 2007). Inlet and outlet each indicates the cross-section in the upstream and downstream where flow comes into and goes out of the flume.

When *O. orca* swim, they maintain certain ranges of submergence depth for efficiency (Williams 2001) and similarly, a scaled and two dimensional *O. orca* is submerged inside the flume at certain depths. Simplification of geometry is inevitable for modeling and to focus on the length of *O. orca*, which is the characteristic parameter among physical properties, complex appearance is simplified as a cross-section of an ellipse having 0.25 ratio between major and minor axis being projected along the width of the flume. The surface of *O. orca* is assumed as no-slip wall to consider the friction between the surface of *O. orca* and the surrounding flow.

Figure 1. Numerical simulation domain and boundary conditions (A) top view of the domain. (B) side view of the domain

The video records of observations present that *O. orca* swim along together in a group, side by side to generate wave, which would overwash a prey lying on the ice floe. If the cooperative action affects only the width of wave and the height and length of waves are equivalent at any lateral location, then the behavior of a whale can represent that of a group except the width of wave. The distance among whales determine whether the shape of hunting wave vary in lateral direction, and to validate, surface profiles behind three *O. orca*s separated by specified distances are obtained in lateral direction from three-dimensional numerical simulation. The result suggests when the distance between *O. orca* does not exceed the width of their body, the surface profiles of wave in lateral direction are almost identical ($R^2 \geq 0.8$) (Fig.2). Since the previous observation shows that *O. orca* stays comparatively close to each other while wave is

washing, it is reasonable to assume three-dimensional effect of each individual whale on the magnitude of wavelength and wave height as negligible. The two-dimensional assumption may be justified by the fact that *O. orca* hunt as group swimming by side-by-side, close to each other.

Figure 2. The influence of distance between *O. orca* on the characteristics of hunting wave. Surface waves are generated behind three *O. orca* separated by specified distance and R^2 between surface profiles are calculated. (A) distance = 0.01 m, $R^2 = 0.82$ (B) distance = 0.02 m, $R^2 = 0.92$ (C) distance = 0.03 m, $R^2 = 0.79$ (D) distance = 0.06 m, $R^2 = 0.61$ (E) distance = 0.09 m, $R^2 = 0.26$. The sub-plot in each figure shows two surface profiles of lowest R^2 for each condition. When the distance between *O. orca* is less than the width of their body (0.03 m), R^2 between surface profiles in lateral direction exceeds 80% (Fig.2A, Fig.2B, Fig.2C). When *O. orca* swims far from each other and the distance reaches twice and three times their body length, R^2 rapidly drops to 60% and 25% (Fig.2D, Fig.2E). Based on the assumption that *O. orca* maintain distance less than their body width with others while 'wave wash', two-dimensional simulation can be justified.

In the nature, hunting waves are generated by swimming of *O. orca* on still water, but for the simulation, it is easier to hold the *O. orca* at one location and let the water flow around it. This strategy has been used in a number of previous studies to analyze the flow structures around marine animals (Lauder *et al.* 2007). Measurements were made after steady state is reached and maintained.

Validation of the CFD Models through Experiment

Experiment was conducted in the hydraulic laboratory at the University of Dundee, UK, having flume tank with a size of 5 m long, 0.08 m wide, and 0.25 m depth with a pump deriving

the flow. An ellipse objects resembling *O. orca* with 0.08 m of width was located in the middle of the flume. The depth of flow was adjusted by installing a vertical wall perpendicular to the flow direction downstream from where the *O. orca* was, thus the velocities were also varied. To measure the magnitude of hunting wave, the picture of water surface was taken with a digital camera(UNIQ), which records 30 frames per second. The software *Digiflow*, analyzed the moves, measuring swimming characteristics and wave parameters (Dalziel 2004). The results of experiments and computational simulation were compared to each other for the purpose of validation.

All measurable wave parameters are compared between the results from the simulations and the laboratory experiments. α, β, γ, z are main wave parameters that validate the simulation results and define the optimal relationship with the swimming behaviors. α is the distance between wave trough and the tail of *O. orca*. β and γ stand for distance from free surface to wave trough and wave crest respectively. z is the distance between wave crest and depth of *O. orca* (Fig.3). Wavelength and wave height are defined by formula based on α, β, γ, z since four wave parameters are not direct estimate of wave magnitude. Free surface profile of simulation show that wave crest appears above *O. orca* near the centerline, and we assume the exact position lies at the right center of *O. orca*. Half of wavelength equals to the horizontal distance from wave crest to wave trough. Based on the assumption of wave crest position, half of wavelength can be estimated as the sum of α and half of *O. orca* length. In other words, $2\alpha + D$ is a proxy distance for wavelength. $\beta + \gamma$ is a proxy distance for the wave height since sum of two parameters approximates the distance from wave trough to wave crest (Fig. 3).

V is the swimming velocity of *O. orca* in nature which is replaced as flow velocity passing through *O. orca* in both simulation and experiment. D is the length of *O. orca* and d is the

swimming depth of *O. orca* (Fig.3). Among the length of the *O. orca* and the depth where whale swims, we have selected the latter along with the velocity to analyze the efficiency of 'wave wash' hunting technique. The velocity and the swimming depth are characteristics that the *O. orca* can adjust while hunting while the length of *O. orca* is innate and inflexible. Since we focus on estimating an effective range of hunting characteristics value, we regard the distance from the free surface to the depth of *O. orca*'s swimming as more suitable length scale to analyze.

Figure 3. Input variables and result parameters of generated wave.

Wave generated by female *O. orca* length of 0.04 m with 5 different velocities (0.33 m/s, 0.35 m/s. 0.40 m/s, 0.45 m/s, 0.49 m/s) and 5 different depths (0.005 m. 0.01 m, 0.015 m, 0.02 m. 0.025 m) are compared between numerical simulation and laboratory experiment.

Results

Simulation results O. orca

The surface waves are generated by a fast moving object in the water, close to the surface by breaking the still surface (Hertel 1966). The simulation result shows that velocity of fluid passing by *O. orca* and their swimming depth determine not only the existence but also the magnitude of wave generated behind *O. orca* (Fig.4). At lowest velocity, change in surface profile is inconspicuous and exact shape of hunting wave is not created (Fig.4A). As velocity increases to 0.35 m/s, hunting wave forms just behind *O. orca*, causing slight disturbance in free surface (Fig.4B). When velocity reaches 0.45 m/s, hunting wave is generated at far behind *O. orca*, and the existence of hunting wave looks more evident (Fig.4C). Swimming depth also influence the characteristics of hunting wave. When *O. orca* is close to free surface, wave

has exact shape consisting clear trough and crest (Fig.4D). The shape of hunting waves become less apparent as depth increases and at d = 0.025m, the amplitude of wave reduces significantly (Fig.4F). It can be inferred that *O. orca* cannot effectively generate waves when they swim too slow or far from free surface.

Figure 4. CFD simulation results showing the surface profile of hunting wave generated at various conditions of d and V. (A) V = 0.15 m/s and d = 0.003 m. (B) V = 0.35 m/s and d = 0.003 m. (C) V = 0.45 m/s and d = 0.003 m. (D) V = 0.15 m/s and d = 0.004 m. (E) V = 0.15 m/s and d = 0.015 m. (F) V = 0.15 m/s and d = 0.025 m. Notice the shape of the generated wave depends on V (panels A, B and C) and d (panels D, E and F).

Experiment results: validation

The result of experiment confirms CFD simulation as suitable method to analyze hunting mechanism of *O. orca*. Wave parameters estimated by two distinct methods, simulation and experiment vary within allowable discrepancy (Fig.5).

Figure 5. Validation of CFD simulation based on experiment results of identical conditions. (A) $\beta+\gamma$ (r^2 = 0.73). (B) z (r^2 = 0.95). Data points resemble the estimated parameter value of experiment on x-axis and simulation on y axis. Dotted lines denote perfect accordance between simulation and experiment result (y = x). r^2 is the value between data points and dotted line.

r^2 of wave height related parameters, z and $\beta+\gamma$, are high enough to confirm high correspondence between experiment and simulation results (Fig.5). On the other hand, α, which is related to the wavelength showed much less r^2 value (r^2 = 0.4). Higher velocity induces larger discrepancy of α between simulation and experiment. Although, α results comparably low r^2, the aspect of change from simulation results regarding the depth and

velocity change agree well to those of the laboratory experiment. Therefore, it is concluded that present numerical simulation method estimates wave height in reasonable and allowable range and suggests wavelength having similar tendency with laboratory experiments.

Estimation of wave parameters

High correlation for z and $\beta+\gamma$ between simulation and experiment results support the feasibility to analyze wave height based on the simulation result. The optimal range of velocity and the swimming depth to achieve the maximum wave height exist as $0.45\ \text{m/s} < V < 0.6\ \text{m/s}$ and $d < 0.005$ m (Fig.6A). When velocity is low, increment of velocity leads to larger wave height, but when velocity exceeds the range of $0.45\ \text{m/s} < V < 0.6\ \text{m/s}$, wave height gradually converges. As *O. orca* swim far from the surface, the hunting wave height continuously decreases.

Simple and efficient equation is derived based on least square regression to represent the combined influence of V and d acting on wave height (Fig. 6B). Here, nondimensional number Fr_d, having d as characteristic length, is introduced for two purposes; both V and d can be expressed at once and analysis become feasible regardless of scale. Fr_d can be explained as a radii of distance influenced by the inertia of moving *O. orca*, in other words, able to propose a threshold value to create surface waves.

$$Fr_d = \frac{V}{\sqrt{gd}} \tag{6}$$

As Fr_d increases, hunting wave height increases and converges later to a certain value. For the small Fr_d, the relationship between Fr_d and the wave height is almost linear. When Fr_d reaches a certain value, wave height grows slowly and finally converges to the constant value

although distance and velocity gradually change. Relationship between Fr_d and wave height is expressed by Eqn.7.

$$\frac{\beta+\gamma}{D} = -0.646\exp(-Fr_d) + 0.43 \quad (7)$$

Wave height converges to $\frac{\beta+\gamma}{D} = 0.43$ when Fr_d is in the range of $2.5 < Fr_d < 3.5$. Additional alteration of velocity and swimming depth do not have effective influence to the wave height in this range.

Eqn.7 can be applied to the wide range of body length of *O. orca* since both Fr_d and $(\beta+\gamma)/D$ are nondimensional numbers. The simulation results demonstrate that nondimensional wave height range in similar values for the same Fr_d, regardless of the body length of *O. orca*.

Figure 6. Analysis of wave height. (A) Contour plot of $(\beta+\gamma)/D$ depending on V and d. (B) $(\beta+\gamma)/D$ as a function of Fr_d for different body length of *O. orca*; ○: female adult, D = 0.04 m; ○: male adult, D = 0.05 m; ○: juvenile, D = 0.02 m. $(\beta+\gamma)/D$ is represented with exponential function as $(\beta+\gamma)/D = -0.646\exp(-Fr_d) + 0.43$ (r^2=0.89). Least square regression between $(\beta+\gamma)/D$ and Fr_d is denoted by dashed line.

The wavelengths are closely related to parameter α, which remains constant with the same velocity, independent from the swimming depth(d) (Fig.7A). It demonstrates that α is the function of only V. Through linear regression, Eqn.8 and Eqn.9 which explain the relationship between α and swimming characteristics of *O. orca*, can be obtained. Due to the discrepancies between simulation and experiment result, data are analyzed respectively with

two independent equations. Based on different velocity range applied to two methods, Eqn.8 obtained from results of numerical simulation is applicable to flow condition of $0.23 < Fr_D < 1.2$, while Eqn.9 from laboratory experiment is applicable to $0.52 < Fr_D < 0.79$

$$\alpha = 0.1834V - 0.0166 \tag{8}$$

$$\alpha = 0.0725V - 0.0189 \tag{9}$$

Figure 7. Analysis of wavelength. (A) Contour plot of α depending on V and d. It indicates that V is the dominant variable. (B) Proxy wavelength, defined as $2\alpha + D$ represented by function of velocity for different body length of *O. orca*; ○: female adult, D = 0.04 m; ○: male adult, D = 0.05 m; ○: juvenile, D = 0.02 m, ✖: experiment data of female adult, D = 0.04 m. Least square regression is denoted by dashed line; ▬ ▬ :numerical simulation ($r^2 = 0.89$); ▬ ▬ :laboratory experiment ($r^2 = 0.41$).

Although wavelength value itself shows the difference between simulation and experiment, the tendency regarding velocity and distance variation corresponds. Fig.8A suggests that wavelength has the positive relationship with the velocity while no significant influence of the distance on wavelength is observed from Fig.8B. Low r-square values in Fig.8B, even lower than 0.1 for both experiment and simulation results justify our assumption applied to the Eqn.8 that α is the function of only V. The experimental results are expected to be more scattered than the numerical simulation due to the unstable experimental conditions. If we consider 99% confidence intervals for both cases, the ranges are overlapping between the data of the numerical simulation and the laboratory experiment.

Figure 8. Relationship between wavelength parameter α and (a) velocity (b) swimming depth of *O. orca*. ○: simulation result ; △: experiment result; ▬ ▬ : linear regression for

simulation result, $\alpha = 0.1565V - 0.0465$; ▬ ▬ : linear regression for experiment result, $\alpha = 0.0725V - 0.0189$. Yellow box represents the overlapped region of 99% confidence intervals between experiment and simulation.

Application to the nature

The average body length of female *O. orca*, 5.6 m, is established as the representative body length to estimate the magnitude of hunting waves in nature and to define the efficient ranges of swimming characteristics, since they play the dominant role to hunt prey by 'wave wash' technique.

For model scale, the wave height converged to maximum value of $\frac{\beta+\gamma}{D} = 0.43$ when two conditions are satisfied; 0.45 m/s $< V <$ 0.6 m/s and 0.003 m $< d <$ 0.005 m (Fig.6). Based on the similarity rule (Street *et al.* 1996), the highest wave height of prototype in nature can be estimated as 2.42 m in the condition of 5.27 m/s $< V <$ 7.04 m/s and 0.41 m $< d <$ 0.68 m by assuming identical Fr_D between model and prototype. In other words, when *O. orca* aims to generate maximum hunting wave maximum height of 2.42 m, it should swim at velocity range of 5.27 m/s $< V <$ 7.04 m/s and depth range of 0.41 m $< d <$ 0.68 m.

Since wavelength is the function of velocity and body length of *O. orca*, considering the previously computed estimated ranges of swimming velocity during hunting, $3.67 m/s \le V \le 7.33 m/s$, and average body length of female *O. orca*, 5.6 m, wavelength in nature vary from 6 ~ 8 m.

The magnitude of wavelength and wave height allows us to compute the total force acting on the prey by vector sum of drag, life and acceleration reaction. For a streamlined body, skin friction drag, which is the tangential force due to viscosity, is dominant compared to the

pressure drag since separation is less likely to occur (Hoerner 1965). When the streamlined body is perfectly symmetric and positioned parallel to the flow direction, the lift coefficient becomes zero (White 2002). For unbroken waves, the acceleration is comparatively small and thus acceleration reaction can be ignored (Denny 1985). Based on the suggested conditions, it leaves us to approximate total force acting on the prey by skin friction drag,

$$F = \frac{1}{2}\rho u^2 C_D S \tag{10}$$

where ρ is the density of sea water, u is horizontal water particle velocity, C_D is the skin friction drag coefficient, and S is the wetted surface area. The Reynolds number corresponding to the surface wave acting on seals ranges from $10^5 \sim 10^6$. C_D for two dimensional streamlined body located in flow of Reynolds number $10^5 \sim 10^6$ range 0.003 - 0.005 (Hoerner 1965) . We approximated constant 0.004 as skin friction drag for corresponding study.

The force can be related to wave parameters by substituting u computed from wave dynamics (Denny 1988). From the linear wave theory, the water particle velocity induced by the wave in deep water at the free surface is

$$u_{\max} = \frac{\pi H}{T} \tag{11}$$

where T is the wave period of hunting wave. Using Eqn.10, the total force is estimated as

$$F = \frac{1}{2}\rho\left(\frac{\pi H}{T}\right)^2 C_D S \tag{12}$$

With $T = \sqrt{\frac{2\pi L}{g}}$ in deep water, where L is the wavelength of hunting wave, the total force

generated by hunting wave imposing on seals can be fully expressed with wave height and wavelength.

$$F = \frac{\pi}{4}\rho g \frac{H^2}{L} C_D S \tag{13}$$

Figure 9. Magnitude of hunting wave in nature scale. (A) Wave height computed by Eqn.7. (B) Total force hunting wave exerts on a seal computed by Eqn.13. Black lines indicate wave magnitude based on equations from numerical simulation and blue lines indicate wave magnitude based on equations from laboratory experiment. ———, d = 0.4 m; – – –, d = 1.1 m; ......, d = 2.5 m; – · – ·, d = 4.5 m. Velocity range are decided based on applicable range of Fr_D for Eqn.8 ($0.23 < Fr_D < 1.2$) and Eqn.9 ($0.52 < Fr_D < 0.79$). Yellow colored area denote estimated velocity range from movie taken by Visser (2007). Purple colored area denotes required wave height and force for successful hunting wave, and green colored area shows the overlapping layer, which would suggest most probable swimming characteristics of *O. orca*.

From Eqn.13, it is shown that as d increases, maximum total force decreases, and velocity corresponding to peak total force increases. For example, from the result obtained from numerical simulation, at $d = 0.4$ m, the have peak force is 113N at 6.9 m/s while at $d = 4.5$ m, the peak force of becomes 66.5N at 18.73 m/s. Solid line on Fig.9B clearly shows that the rate of increase before reaching the maximum value is steeper than rate of decrease after reaching the maximum value. Result from laboratory experiment shows similar trends with numerical simulation but the values are larger than those from numerical simulation. (Fig.9B). Ranges of velocity and swimming depth corresponding to probable swimming characteristics of *O. orca* is identical regardless of method of analysis.

Discussion

The efficient 'wave wash' hunting technique

The success of 'wave wash' hunting technique is determined by wave height and force imposed on the prey which depend on swimming velocity and swimming depth of *O. orca*. Dimension of the prey, crabeater seal is estimated as the length of 2 m, and the height of 1.0 m (Siniff and Bengtson 1977). Width is not considered due to the two-dimensional assumption in the numerical and laboratory experiments.

Successful hunting wave occurs when overtopping condition is satisfied and wave height exceed the height of target object, for this case, crabeater seal lying on the floating ice (1.0 m). Although *O. orca* can generate hunting wave of height 2.42 m in maximum, previous research show that typical hunting wave height generated by *O. orca* is 1.0 m, reaching the minimum wave height to generate successful 'wave wash' (Pitman and Durban 2012). When d is 0.4 m, there is no minimum velocity required to exceed wave height of 1.0 m. At larger d of 1.1 m, required minimum velocity appears to be 3.3 m/s. When d increases to 2.5 m and 4.5 m required minimum velocity increases to 5.0 m/s and 6.4 m/s respectively (Fig.9A). Previous research suggest that surface waves becomes hard to distinguish when the swimmer submerges to a depth exceeding three body diameters (Williams 2000). Distance of 4.5 m approximates three body diameters of *O. orca* and wave height corresponding to $d = 4.5$ m do not exceed 1.0 m for average range of swimming velocity of *O. orca*, showing identical results with previous research.

Another crucial wave characteristic to define success of hunting wave is the total force acting on the prey, which demonstrates how strongly hunting wave pushes seals to cause overwash. Powerful force is not generated by high swimming speed, but rather speed of finite range corresponding to each depth of *O. orca* from the free surface (Fig.9B).

The resisting force of seals establish minimum force required to push seals until the edge of ice floe to cause wave wash. The friction would impede movement of seals, and determine the magnitude of resisting force as

$$F_f = \mu_k N \tag{14}$$

where μ_k is the coefficient of friction between seals and ice and N is normal force, in other words, weight of seals. From physical intuition, wave wash occurs when total force of hunting wave surpasses the resisting force of seals (Buckley *et al.* 2010). If $F_D \geq F_f$, total force of wave is sufficient enough to cause wave wash, pushing seal to the edge of ice and making them to fall into the sea. Approximating $\mu_k = 0.2$ (Frederking and Barker 2002) and weight of seals as 300 N (Laws *et al.* 2003), at least 60 N of wave force should be generated for successful hunting which is marked by purple colored area in Fig.9. For d = 0.4, 1.1, 2.5, 4.5 m, drag force exceed 60 N at velocity 2.7 ~ 3 m/s$\leq V$, 4.5 ~ 5.0 m/s$\leq V$, 7 ~ 8.5 m/s$\leq V$, 9.5 ~ 13.5 m/s$\leq V$ in sequence. Regarding actual swimming speed of *O. orca*, suitable range of d to reach minimum total force confines to 0.4 m$\leq d \leq$1.1 m/s (Fig.9B).

It is evident that large and powerful wave would result more successful 'wave wash', but in general requires *O. orca* to swim fast close to the surface. Metabolic rate linearly increases as velocity increases (Guinet et al 2007) and the drag force *O. orca* experience increase as they swim close to the free surface (Lang and Daybell 1963). In other words, *O. orca* invest least effort on swimming when they swim slow, far from the surface. By considering both success and energy invested during hunting, the most efficient range of swimming characteristics for 'wave wash' hunting technique would be 3 m/s$\leq V \leq$5 m/s and 0.5 m$\leq d \leq$1.1 m.

Among diverse hunting mechanism of *O. orca*, the 'wave wash' technique is unique that *O. orca* seek to hunt prey originally located outside of water by making the prey to drown.

'Intentional stranding' is another hunting technique of *O. orca* to hunt prey outside of water, but encompasses risk that *O. orca* should be skillful enough to return to offshore after seizing the prey at onshore (Guinet 1990, Guinet and Bouvier 2004). Most frequent hunting strategy encompass chase and attack. Previous studies indicate the swimming velocity of *O. orca* range between 4 - 9 m/s while chasing the prey depending on the duration time of swimming, which usually lasts for 30 - 60 min (Guinet et al 2007, Ford 2005). Compared to the swimming velocity required for successful 'wave wash', the chasing velocity is faster and demands higher metabolic rate (Guinet et al 2007). To attack, *O. orca* exhibit diverse tactics. When the preys are moving in groups, *O. orca* generate waves to dismiss the group and isolate one of them which would become the target of hunting (Pitman *et al.* 2001). The final step of diverse hunting mechanism is identical that *O. orca* damage the prey and lead them to death. *O. orca* toss their prey into the air with their tails until prey are severely wounded (Reyes and Borboroglu 2004), pull apart the prey at opposite locations by cooperation to rip apart the prey body and strike the prey with tail or flippers (Baird and Dill 1995). In the respect that 'wave wash' hunting strategy do not accompany risk and can be achieved without chasing the prey for long period of time by drowning the prey originally located outside of water, it is comparatively efficient and safe among diverse hunting mechanisms of *O. orca*.

Conclusion

In order to quantitatively analyze the hunting mechanism of *O. orca*, we have carried out CFD simulations and proposed empirical equations that decide the wavelength (Eqn.8 and Eqn.9) and wave height (Eqn.7) of the hunting wave as functions of the swimming speed and the depth of *O. orca*, respectively. Wave height of 1.0 m and drag force of 60N were selected as standards of successful hunting wave and the linear wave theory provided a foundation to calculate ranges of swimming velocity ($3\ \text{m/s} \leq V$) and depth ($0.4\ \text{m} \leq d \leq 1.1\ \text{m}$) of *O. orca* to

generate successful hunting wave.

We assessed the efficiency of the hunting behavior of *O. orca* by two criteria: (1) if hunting waves are of proper magnitude and (2) if the swimming motion is economical. The threshold values of successful hunting waves are defined above, and the wave height and the resulting force exceeding but close to the threshold values would be the most suitable and efficient magnitude of hunting waves. Economical swimming for *O. orca* is to invest less effort to achieve the goal of locomotion. If *O. orca* experience less disturbance to move forward and succeed hunting, they consume less effort to that extent, which can be classified as economical swimming. In this regard, it is most efficient to swim slow at submerged location among velocity and distance ranges required to achieve successful hunting wave. From our analysis, the most efficient hunting process can be defined as *O. orca* swimming in the ranges of 3 m/s $\leq V \leq$ 5 m/s and 0.5 m $\leq d \leq$ 1.1 m to generate hunting wave of height 1.0 m $\leq H$ and wave drag force of 60 N $\leq F_D$.

Our definition of efficient hunting process estimated by physical approach based on CFD simulation and the linear wave theory suggests more specific ranges of required swimming characteristics compared to observation data and helps to better understand the 'wave wash' hunting process of *O. orca*.

Acknowledgement

This research was supported by the Polar Academic Program (PE18900) of the Korea Polar Research Institute, the Basic Science Research Program through the National Research Foundation of Korea (NRF) funded by the Ministry of Science, ICT & Future Planning (NRF-2017R1A2B4007977), and administratively supported by the Institute of Engineering Research at Seoul National University.

Literature cited

Alex Shorter, K., Murray, M. M., Johnson, M., Moore, M., and Howle, L. E. 2014. Drag of suction cup tags on swimming animals: modeling and measurement. Marine Mammal Science 30.2: 726-746.

Alexander, R., and Jayes, A. S. 1983. A dynamic similarity hypothesis for the gaits of quadrupedal mammals. Journal of zoology 201.1: 135-152.

Anderson, F. E. 2002. Effect of wave-wash from personal watercraft on salt marsh channels. Journal of Coastal Research: 33-49.

Baird, R. W., and Dill, L. M. 1995. Occurrence and behaviour of transient killer whales: seasonal and pod-specific variability, foraging behaviour, and prey handling. Canadian Journal of Zoology 73.7: 1300-1311.

Baird, R. W., and Dill, L. M. 1996. Ecological and social determinants of group size in transient killer whales. Behavioral Ecology 7.4: 408-416.

Bonham, A. J. 1983. The management of wave-spending vegetation as bank protection against boat wash. Landscape planning 10.1: 15-30.

Buckley, M. L., Wei, Y., Jaffe, B. E., and Watt, S. G. 2012. Inverse modeling of velocities and inferred cause of overwash that emplaced inland fields of boulders at Anegada, British Virgin Islands. Natural Hazards 63.1: 133-149.

Bushnell, D. M., and Moore, K. J. 1991. Drag reduction in nature. Annual Review of Fluid Mechanics 23.1:65-79.

Dalziel, S. B. 2004. Digiflow user manual.

De Waal, J. P., and Van der Meer, J. W. 1993. Wave runup and overtopping on coastal

structures. Coastal Engineering 1992: 1758-1771.

Denny, M. A. R. K. 1999. Are there mechanical limits to size in wave-swept organisms? Journal of Experimental Biology 202.23: 3463-3467.

Donnelly, C., Ranasinghe, R., and Larson, M. 2006. Numerical modeling of beach profile change caused by overwash. In Coastal Dynamics 2005: State of the Practice: 1-14.

Dumont, D., Kohout, A., and Bertino, L. 2011. A wave□based model for the marginal ice zone including a floe breaking parameterization. Journal of Geophysical Research: Oceans 116.C4.

Ford, J. K., Ellis, G. M., Matkin, D. R., Balcomb, K. C., Briggs, D., and Morton, A. B. 2005. Killer whale attacks on minke whales: prey capture and antipredator tactics. Marine mammal science 21.4: 603-618.

Fish, F. E. 1998. Comparative kinematics and hydrodynamics of odontocete cetaceans: morphological and ecological correlates with swimming performance. Journal of Experimental Biology 201.20: 2867-2877.

Fish, F. E., and Rohr, J. J. 1999. Review of dolphin hydrodynamics and swimming performance. No. SPAWAR/CA-TR-1801. Space and naval warfare systems commandSan Diego CA.

Fish, F. E. 2000. Biomechanics and energetics in aquatic and semiaquatic mammals: platypus to whale. Physiological and Biochemical Zoology 73.6: 683-698.

Fish, F. E., and Lauder, G. V. 2006. Passive and active flow control by swimming fishes and mammals. Annu. Rev. Fluid Mech. 38: 193-224.

Frederking, R. J., and Barker, A. 2002. Friction of sea ice on steel for condition of varying speeds. In The Twelfth International Offshore and Polar Engineering Conference.

International Society of Offshore and Polar Engineers.

Gaylord, B., and Denny, M. 1997. Flow and flexibility. I. Effects of size, shape and stiffness in determining wave forces on the stipitate kelps *Eisenia arborea* and *Pterygophora californica*. Journal of Experimental Biology 200.24: 3141-3164.

Guinet, C. 1991. Intentional stranding apprenticeship and social play in killer whales (*Orcinus orca*). Canadian Journal of Zoology 69.11:2712-2716.

Guinet, C., and Bouvier, J. 1995. Development of intentional stranding hunting techniques in killer whale (*Orcinus orca*) calves at Crozet Archipelago. Canadian Journal of Zoology 73.1:27-33.

Guinet, C., Domenici, P., De Stephanis, R., Barrett-Lennard, L., Ford, J. K. B., and Verborgh, P. 2007. Killer whale predation on bluefin tuna: exploring the hypothesis of the endurance-exhaustion technique. Marine Ecology Progress Series 347: 111-119.

Hazekamp, A. A., Mayer, R., and Osinga, N. 2010. Flow simulation along a seal: the impact of an external device. European Journal of Wildlife Research 56.2: 131-140.

Hedenström, A., and Alerstam, T. 1995. Optimal flight speed of birds. Phil. Trans. R. Soc. Lond. B 348.1326:471-487.

Hertel, H. 1966. Structure, form, movement.

Hoerner, S. F. 1965. Fluid-dynamic drag: theoretical, experimental and statistical information. Hoerner Fluid Dynamics.

Jacobsen, N. G., Fuhrman, D. R., and Fredsøe, J. 2012. A wave generation toolbox for the open□source CFD library: OpenFoam®. International Journal for Numerical Methods in Fluids 70.9:1073-1088.

Jefferson, T. A., Stacey, P. J., and Baird, R. W. 1991. A review of killer whale interactions with other marine mammals: Predation to co□existence. Mammal review 21.4:151-180.

Lang, T. G., and Daybell, D. A. 1963. Porpoise performance tests in a sea-water tank. No. NOTS-TP-3063. NAVAL ORDNANCE TEST STATION CHINA LAKE CA.

Lauder, G. V., Anderson, E. J., Tangorra, J., and Madden, P. G. 2007. Fish biorobotics: kinematics and hydrodynamics of self-propulsion. Journal of experimental biology 210.16:767-2780.

Laws, R. M., Baird, A., and Bryden, M. M. 2003. Size and growth of the crabeater seal *Lobodon carcinophagus* (Mammalia: Carnivora). Journal of Zoology 259.1:103-108.

Pavlov, V. V., and Rashad, A. M. 2012. A non□invasive dolphin telemetry tag: computer design and numerical flow simulation. Marine Mammal Science 28.1.

Pitman, R. L., Ballance, L. T., Mesnick, S. I., and Chivers, S. J. 2001. Killer whale predation on sperm whales: observations and implications. Marine mammal science 17.3:494-507.

Reyes, L. M., and García-Borboroglu, P. 2004. Killer whale (*Orcinus orca*) predation on sharks in Patagonia, Argentina: a first report. Aquatic Mammals 30.3:376-379.

Rohr, J. J., and Fish, F. E. 2004. Strouhal numbers and optimization of swimming by odontocete cetaceans. Journal of Experimental Biology 207.10:1633-1642.

Siniff, D. B., and Bengtson, J. L. 1977. Observations and hypotheses concerning the interactions among crabeater seals, leopard seals, and killer whales. Journal of Mammalogy 58.3:414-416.

Vennell, R., Pease, D., and Wilson, B. 2006. Wave drag on human swimmers. Journal of biomechanics 39.4:664-671.

Watts, P., and Fish, F. E. 2001, August. The influence of passive, leading edge tubercles on wing performance. In Proc. Twelfth Intl. Symp. Unmanned Untethered Submers. Technol. Durham New Hampshire: Auton. Undersea Syst. Inst.

Weihs, D. 1973. Optimal fish cruising speed. Nature 245.5419:48.

White, F. M. 1986. Fluid mechanics. McGraw-hill.

Wilga, C. D., Maia, A., Nauwelaerts, S., and Lauder, G. V. 2012. Prey handling using whole-body fluid dynamics in batoids. Zoology 115.1:47-57.

Williams, T. M. 2001. Intermittent swimming by mammals: a strategy for increasing energetic efficiency during diving. American Zoologist 41.2:166-176.

Williams, T. M. 2009. Swimming. In Encyclopedia of Marine Mammals (Second Edition) :1140-1147.

Table 1.

	Prototype	Model
Length (m)	5.6	0.04
Velocity (m/s)	3.67 ~ 7.33	0.15 ~ 0.75
Froude number	0.41 ~ 0.95	0.23 ~ 1.19
Weber number	$0.73 \sim 3.95 \times 10^{6}$ (1)	$0.13 \sim 3.29 \times 10^{2}$ (1)

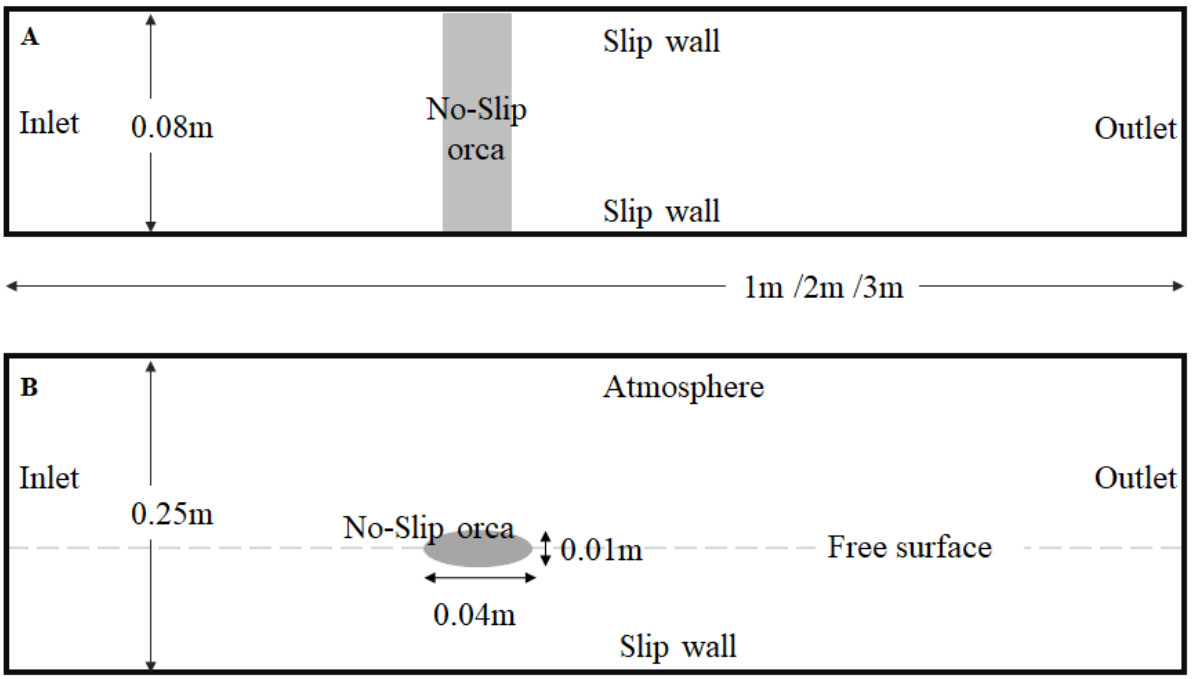
A
Slip wall
Inlet
0.08m
No-Slip
orca
Outlet
Slip wall
1m /2m /3m
B
Atmosphere
Inlet
Outlet
0.25m
No-Slip orca
0.01m
Free surface
0.04m
Slip wall

Figure 1

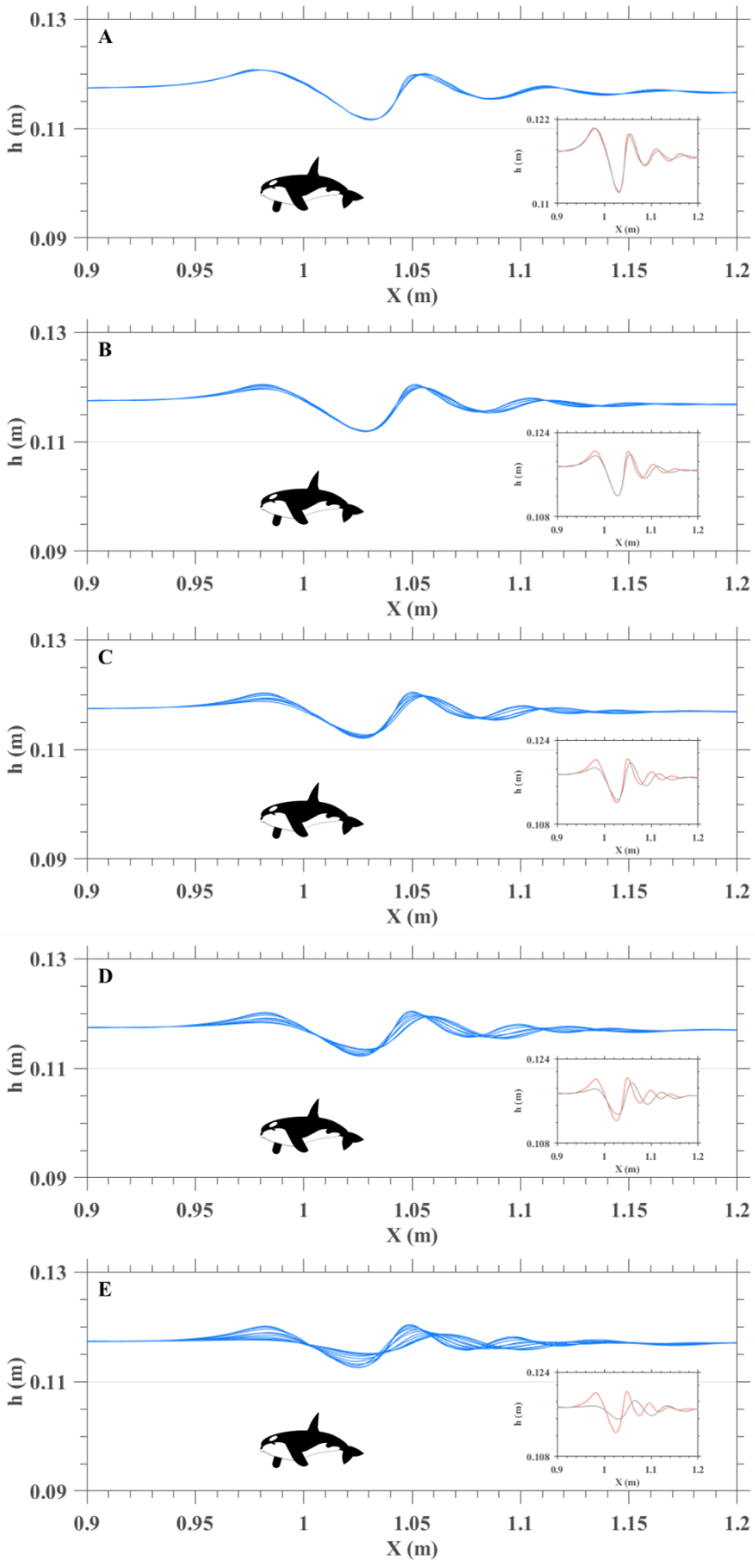

Figure 2

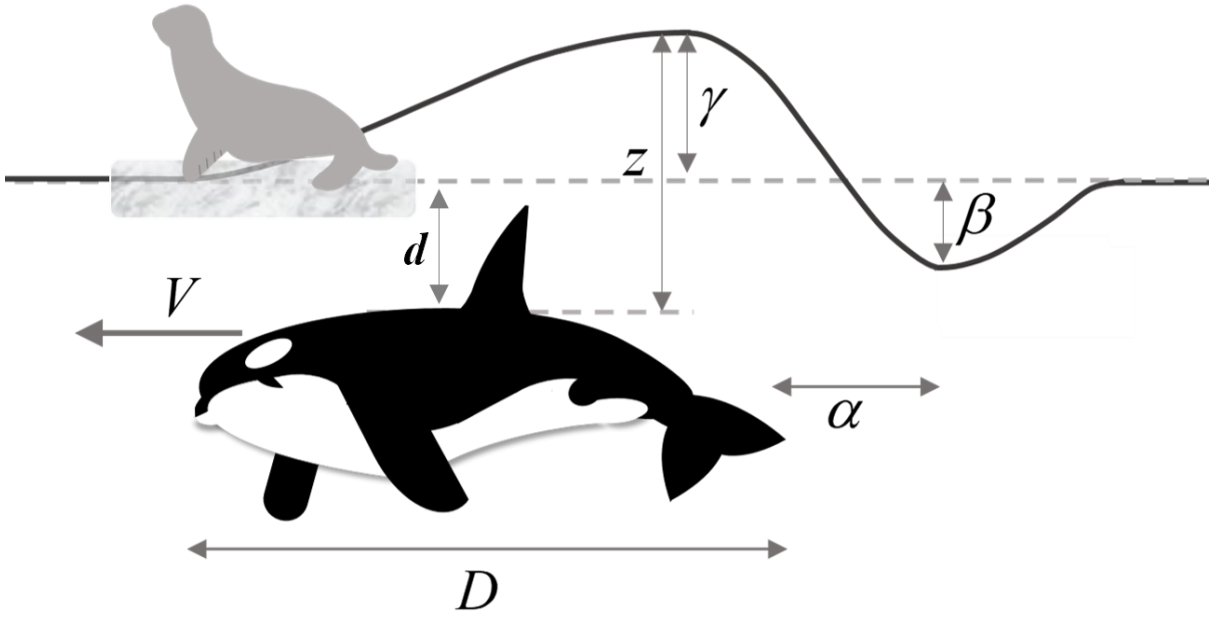

Figure 3

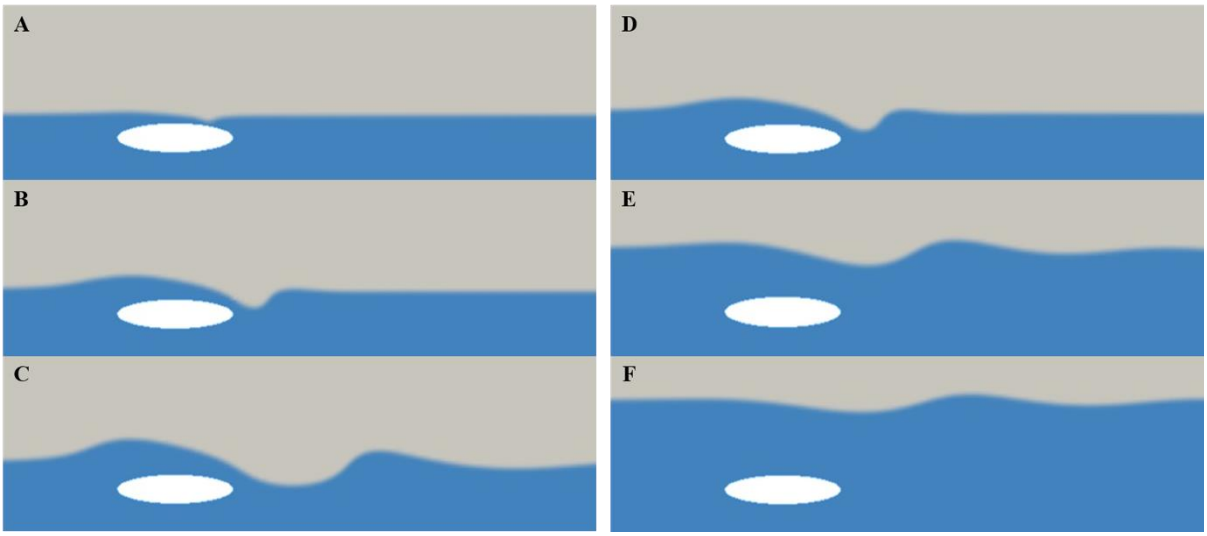

Figure 4

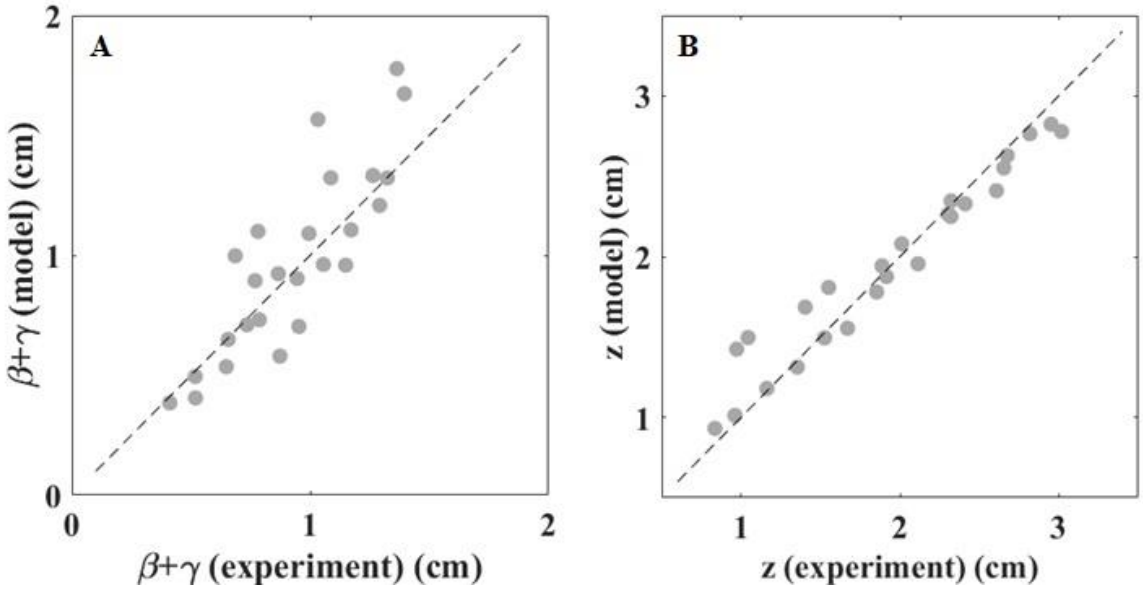
A
B
β+γ (model) (cm)
β+γ (experiment) (cm)
z (model) (cm)
z (experiment) (cm)
0
1
2
3

Figure 5

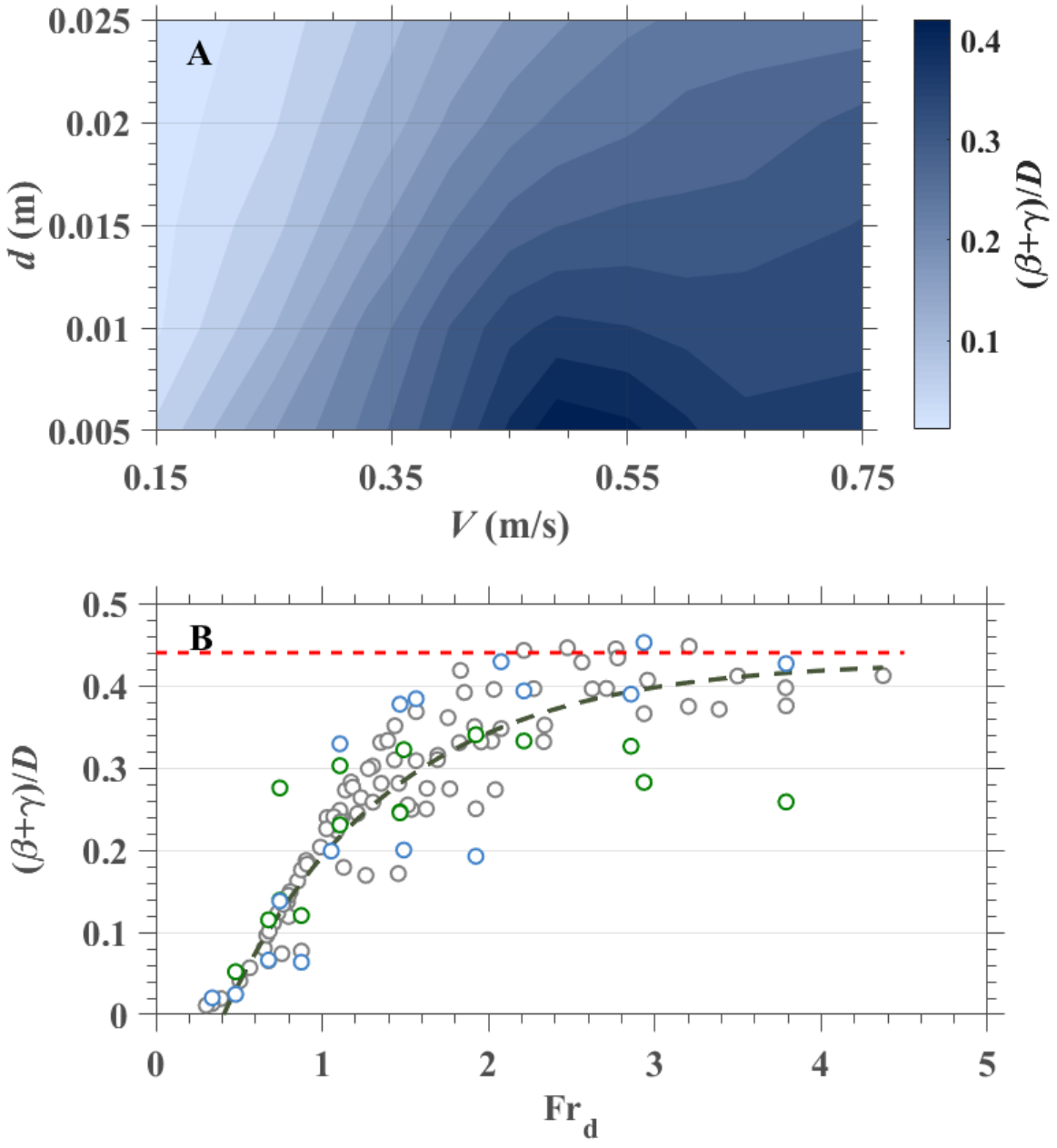
A
0.025
0.02
0.015
0.01
0.005
d (m)
0.15
0.35
0.55
0.75
V (m/s)
0.4
0.3
0.2
0.1
(β+γ)/D
B
0.5
0.4
0.3
0.2
0.1
0
(β+γ)/D
0
1
2
3
4
5
Fr d

Figure 6

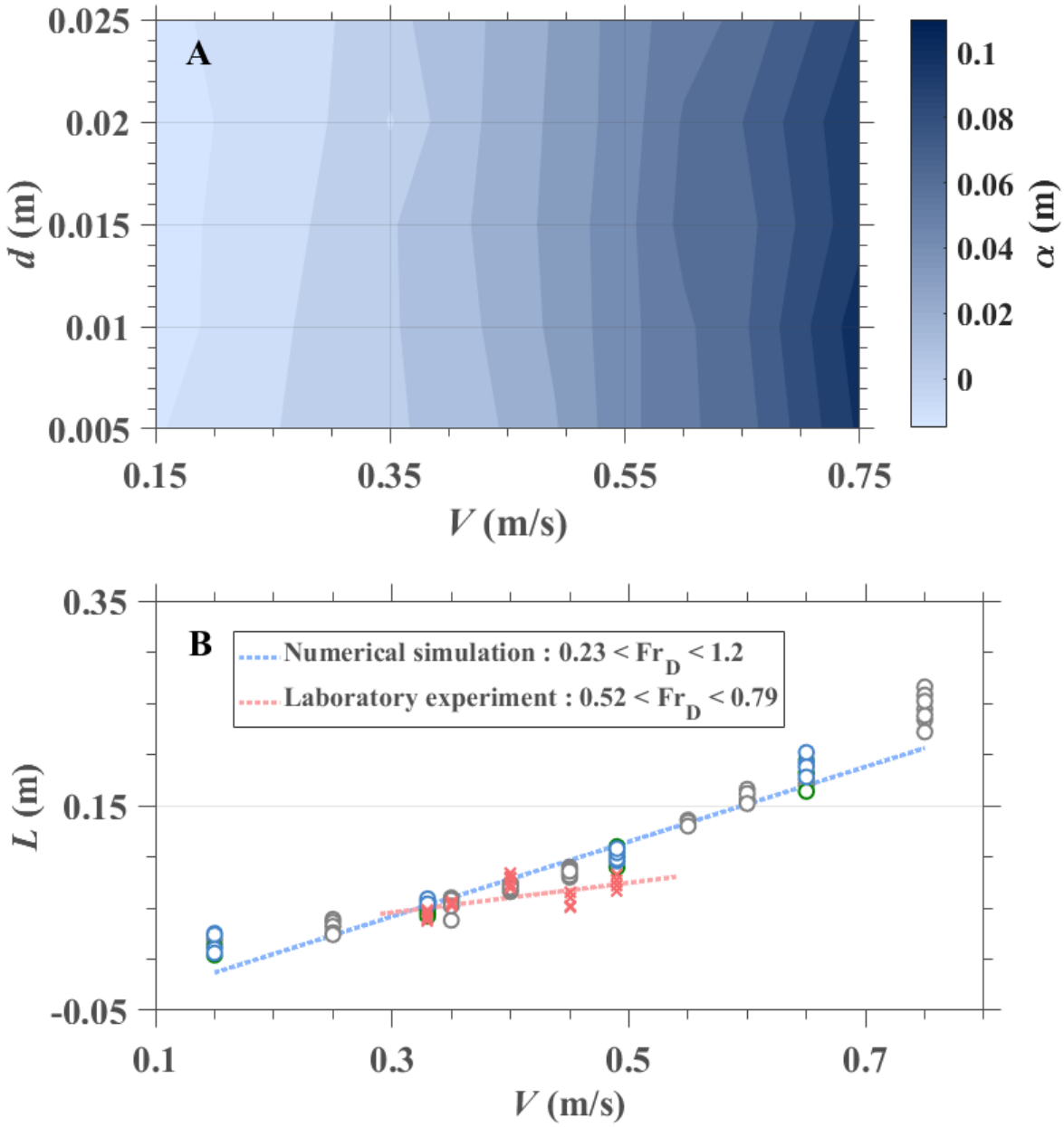
A
0.025
0.02
0.015
0.01
0.005
d (m)
0.15
0.35
0.55
0.75
V (m/s)
0.1
0.08
0.06
0.04
0.02
0
α (m)
B
Numerical simulation : 0.23 < Fr_D < 1.2
Laboratory experiment : 0.52 < Fr_D < 0.79
0.35
0.15
-0.05
L (m)
0.1
0.3
0.5
0.7
V (m/s)

Figure 7

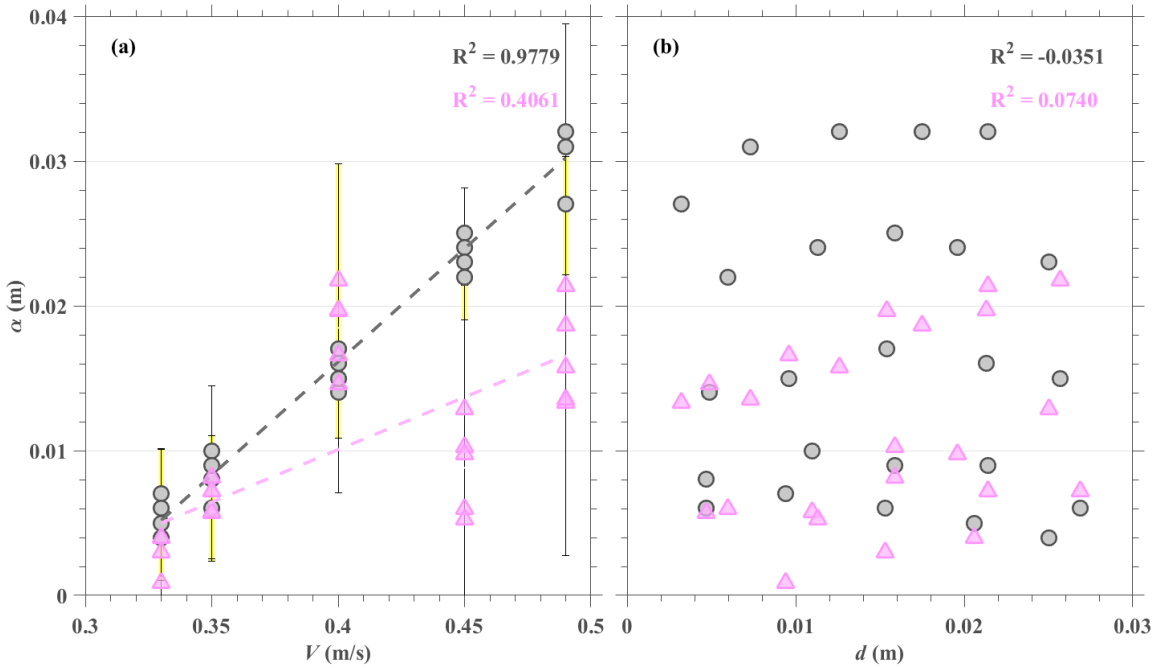

Figure 8

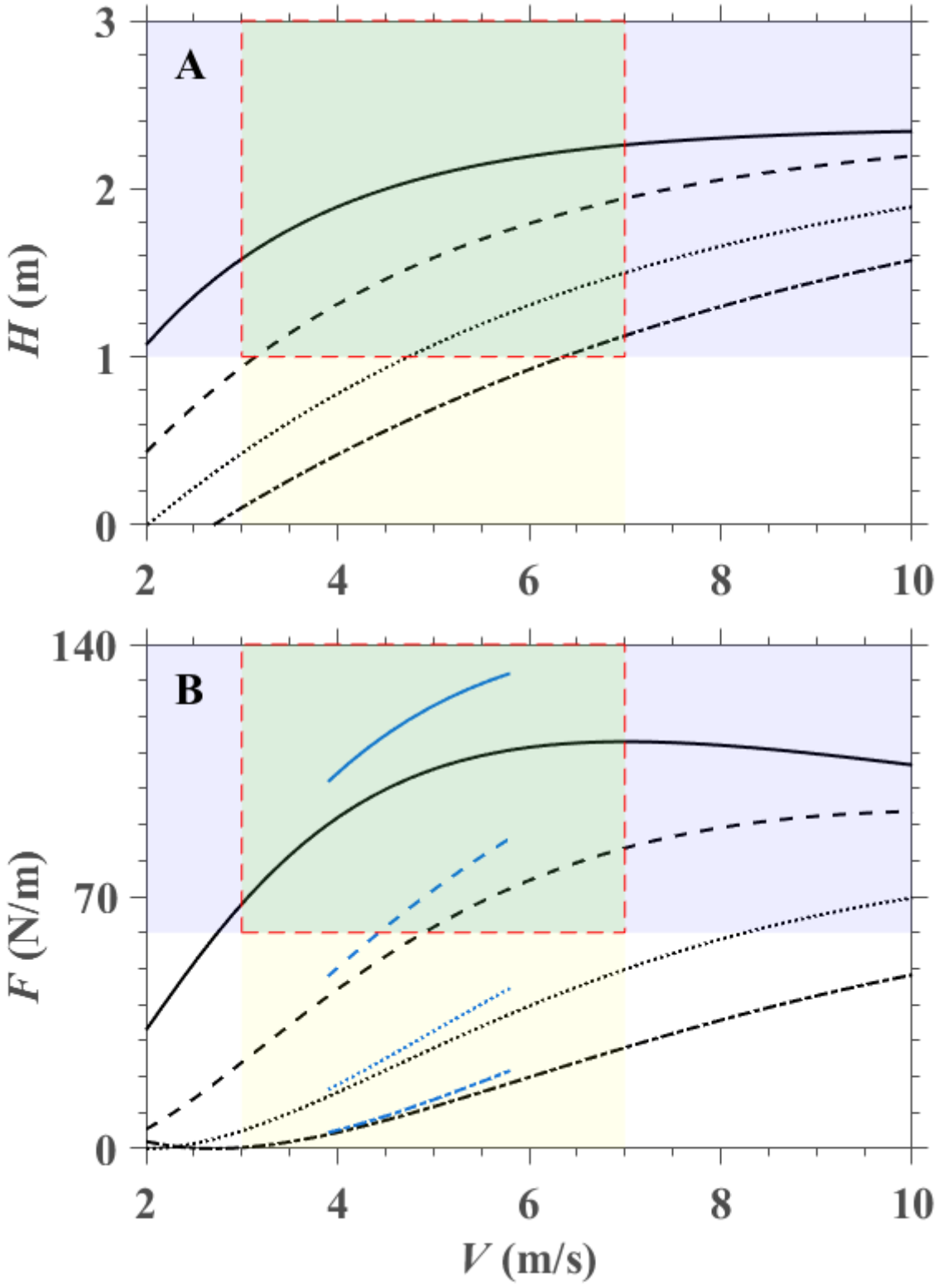

Figure 9